

Formation and thermal stability of quasi-amorphous thin filmsV. Lyahovitskaya,¹ Y. Feldman,² I. Zon,¹ E. Wachtel,² K. Gartsman,² A. K. Tagantsev,³ and I. Lubomirsky^{1,*}¹*Department of Materials & Interfaces, Weizmann Institute of Science, Rehovot 76100, Israel*²*Chemical Research Support Unit, Weizmann Institute of Science, Rehovot 76100, Israel*³*Department of Materials Science, Ecole Polytechnique Federale De Lausanne, Switzerland*

(Received 28 July 2004; published 23 March 2005)

The thermal stability of amorphous ionic solids is usually attributed to kinetic considerations related to mass transport. However, there are a number of amorphous ionic solids, which have recently been described, whose unusual resistance to nucleation and subsequent crystallization cannot be explained by mass transport limitations. Examples have been found in a large variety of fields, spanning the range from thin solid films to biomineralization. This poses a question regarding a possible common mechanism for the stabilization of amorphous ionic solids. Here we present a model which explains the formation and thermal stability of quasi-amorphous thin films of BaTiO₃, one of the amorphous systems recently described which exhibit unusual thermal stability. On the basis of the experimental evidence presented we suggest that nucleation of the crystalline phase can occur only if the amorphous phase undergoes volume expansion upon heating and transforms into an intermediate low density amorphous phase. If volume expansion is unobstructed by external mechanical constraints, nucleation proceeds freely. However, thin films are clamped by a substrate; therefore, volume expansion is restricted and the low-density intermediate phase is not formed. As a result, under certain conditions, nucleation may be completely suppressed and the phase which appears is quasi-amorphous. A quasi-amorphous film is under compressive stress and as long as the mechanical constraints are in place it remains stable at the temperatures that normally lead to crystallization of amorphous BaTiO₃. Quasi-amorphous thin films of BaTiO₃ exhibit pyroelectricity, the origin of which is also explained by the proposed model.

DOI: 10.1103/PhysRevB.71.094205

PACS number(s): 61.43.Er, 64.70.Nd

I. INTRODUCTION

The subject of the thermal stability of amorphous ionic solids has attracted considerable interest recently in a broad variety of fields spanning the range from thin solid films^{1,2} to biomineralization.³ In contrast to glasses, amorphous ionic solids do not contain an extended network of bonds which form the glassy state. Instead these solids are usually viewed as random closed-packed structures⁴ (RCP) that are kinetically stabilized. This kinetic stabilization is generally attributed to diffusion limitations that obstruct the nucleation process. The more atoms there are in the unit cell, the more pronounced is the effect. Therefore, amorphous ionic solids are more stable if the structure resulting from crystallization has many atoms per unit cell or has stoichiometry that is different from the stoichiometry of the amorphous matrix. In both cases, formation of a nucleus requires rearrangement of a large number of atoms and therefore may occur only at elevated temperature.

However, over the last few years there has been increasing evidence^{1,3,5-8} that there are noncrystalline ionic solids whose relatively high resistance to nucleation and subsequent crystallization cannot be explained by mass transfer limitations. Amorphous ionic solids like CaCO₃ and BaTiO₃ may remain noncrystalline at a temperature which would normally cause crystallization.^{3,6,7} The unit cells of crystalline CaCO₃ and BaTiO₃ contain very few atoms, and the compositions of the amorphous solids are identical to that of the corresponding crystalline phases. Thus diffusion limitations cannot explain their resistance to nucleation and subsequent crystallization. Therefore, finding a mechanism that may account for this effect would constitute substantial

progress. Here we present a model that provides a satisfactory explanation for the thermal stability of one ionic solid, the recently described quasi-amorphous BaTiO₃.

It has been reported recently⁶ that amorphous BaTiO₃ thin films prepared by radio frequency (rf) magnetron sputtering do not crystallize if pulled through a temperature gradient with peak temperature of 600 °C. Instead, they form a phase which is not crystalline according to x-ray and electron diffraction (XRD, ED), but which is thermally stable below 800 °C. This phase exhibits significant pyroelectric and piezoelectric effects (>10% of that for bulk BaTiO₃), indicating that the structure is polar. Following Ref. 6 this phase will be henceforth referred to as quasi-amorphous. The transformation of the as-deposited amorphous films to the quasi-amorphous state is accompanied by the development of a high in-plane compressive stress,⁶ whereas amorphous as-deposited films are stress free and neither pyroelectric nor piezoelectric. The dielectric constant of as-deposited amorphous films is ≈9–12 but it increases to ≈30–32 after transformation into the quasi-amorphous state. This increase of the dielectric constant led to the suggestion that the polarity of the quasi-amorphous phase is related to the formation and ordering of crystal motifs,⁹ regions with local order that decays within two to three coordination spheres.¹⁰ These considerations, along with the experimental observations, provide a basis for a phenomenological description of the phenomenon. BaTiO₃ is >85% ionic¹¹ and is not known to form stable glass phases under any conditions. This poses a question regarding the mechanism by which a noncrystalline ionic solid can be thermally stable and acquire and retain polarity. This work attempts to address these issues.

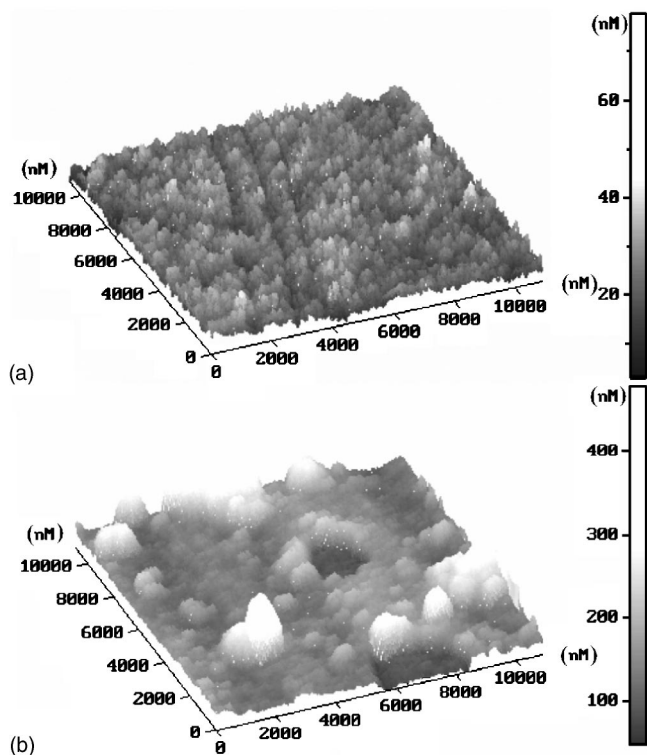


FIG. 1. AFM profiles of an as-deposited amorphous film that (a) forms a quasi-amorphous phase after pulling through the temperature gradient and (b) crystallizes after pulling through the temperature gradient.

II. EXPERIMENT

Amorphous 100–250-nm-thick films of BaTiO₃ were deposited by rf sputtering on bare Si or on Si covered with a 20-nm-thick MgO seeding layer. Details of the film deposition procedure have been described earlier.⁶ As-deposited films were either pulled (2–5 mm/h) through a temperature gradient with peak temperature of 600–700 °C or annealed under isothermal conditions at 600–800 °C for 20–120 min.⁶ Several as-deposited amorphous films were converted to substrate-free 200×200 μm² films^{12,13} which remained tethered at their edges. These were then subjected to heat treatments identical to those of the substrate-supported films. Transmission electron microscopy (TEM, Phillips CM-120) combined with ED and XRD was used to analyze film structure. Scanning electron microscopy (Phillips XL30 ESEM-FEG) was employed to image film surfaces and cross sections. Surface roughness of the films was measured with atomic force microscopy (NT-MDT LP7).

III. RESULTS

The crystallization kinetics of the as-deposited amorphous BaTiO₃ films strongly depends on the initial film quality (presence of inclusions, voids and surface roughness), on the type of thermal treatment, and on the presence or absence of a MgO seeding layer. The standard deposition procedure yields films that are dense and uniform and have a minimum concentration of macroscopic defects [Figs. 1(a) and 2(a)].

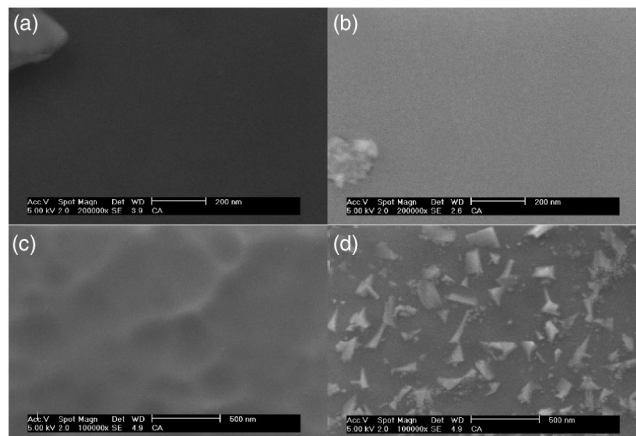


FIG. 2. SEM images of (a) as-deposited amorphous BaTiO₃ film without detectable structural defects and surface roughness <20 nm, (b) the film shown in (a) after pulling through the temperature gradient with a maximum temperature of 600 °C, (c) as-deposited amorphous BaTiO₃ film with surface roughness >50 nm, and (d) the film shown in (c) after pulling through the temperature gradient with a maximum temperature of 600 °C. The crystals which appeared at the surface serve as crystallization centers during further heat treatment and eventually cause complete crystallization of the amorphous phase. For (a) and (b) the areas with dust particles stuck to the surface enabled proper focusing, which is not possible otherwise.

These films have a surface roughness of <20 nm. Pulling through the temperature gradient converts as-deposited amorphous films into the quasi-amorphous state. Subsequent heat treatment up to 800 °C does not lead to crystallization of these films, irrespective of the type of treatment: multiple passes through the gradient or annealing under isothermal conditions (Fig. 2). As-deposited films with a large number of structural defects [Fig. 1(b)] and/or surface roughness greater than 50 nm crystallize after pulling through the temperature gradient [Fig. 2(d)]. The films deposited on MgO seeding layers undergo crystallization into randomly oriented BaTiO₃ irrespective of the type of heat treatment. All the as-deposited films crystallize if placed in a temperature of 600 °C or higher, irrespective of the substrate type or presence of structural defects. The appearance of the crystalline phase can be detected already after 30 min at 600 °C.

XRD patterns of the quasi-amorphous films are identical to those of the as-deposited films and reveal no diffraction peaks.⁶ ED patterns of the as-deposited films and quasi-amorphous films show a diffuse ring at 3.17(±0.1) Å and, rarely, a second ring, which is too broad to be assigned a specific location (Fig. 3). Transformation of the as-deposited films into the quasi-amorphous state is accompanied by large changes in the refractive index, birefringence, dielectric constant, and mechanical stress⁶ (Table I). The density of the as-deposited amorphous, quasi-amorphous, and polycrystalline films (Table I) deduced from the refractive index data suggests that the specific volume increases during transformation of the as-deposited amorphous films into the quasi-amorphous or into the polycrystalline state. Further verifi

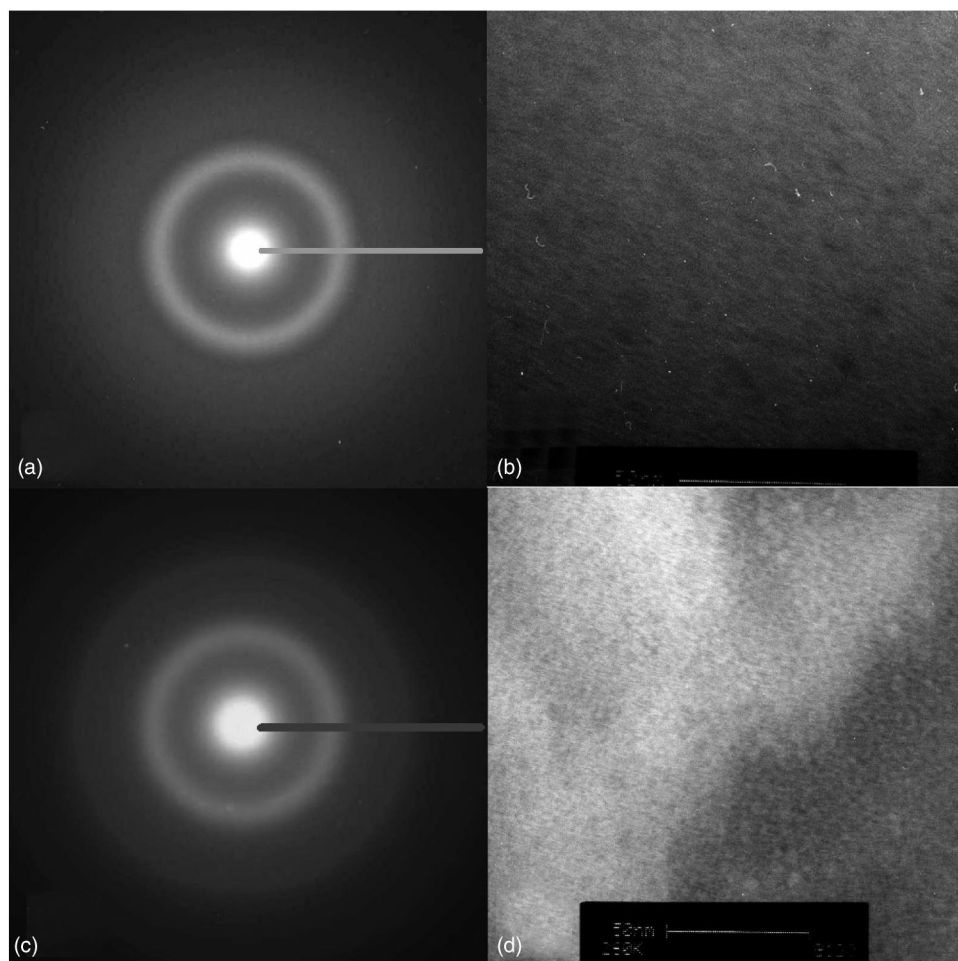
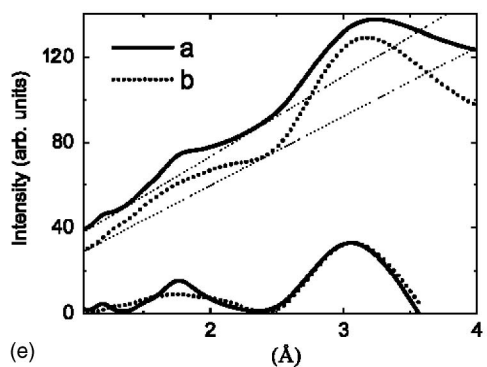


FIG. 3. TEM investigation the amorphous and quasi-amorphous films: (a) and (c) electron diffraction (ED) patterns of amorphous and quasi-amorphous films, respectively, (e) intensity profiles of the ED patterns (upper lines) and the profiles after subtraction of the linear background (lower lines), and (b) and (d) TEM images of amorphous and quasi-amorphous films, respectively. The scale bar is 50 nm, electron beam sampling area 5 μm .



cation of this fact comes from experiments with substrate-free films. These films of as-deposited amorphous BaTiO_3 are flat but expand and corrugate after heat treatment. The expansion of the substrate-free films becomes noticeable at 200 °C (Fig. 4) and progresses until 470 °C, above which nucleation starts. From the height of the corrugation pattern measured by optical microscopy¹³ the degree of expansion of the substrate-free films was calculated to be within the range of 6%–15%, too large to be explained by thermal expansion. The time period over which the expansion occurs depends on temperature and comprises <60 min at 450 °C and <120 min at 250 °C.

IV. DISCUSSION

Three types of films were investigated: (1) dense, smooth, and uniform films, (2) films with a large number of structural defects and/or large surface roughness, and (3) films deposited on a MgO seeding layer. The quasi-amorphous state forms only if dense, smooth, and uniform films are pulled through the temperature gradient. In this regard one can define three issues that are central for the understanding of the quasi-amorphous state: (a) there are conditions under which crystallization of amorphous BaTiO_3 is completely suppressed, (b) the quasi-amorphous phase, once formed, is stable at temperatures that would normally lead to crystalli-

TABLE I. Properties of BaTiO₃ thin films compared with the properties of bulk BaTiO₃. n_{\perp} is the refractive index in the direction perpendicular to the film plane, n_{\parallel} is the refractive index in the direction parallel to the film plane, and n_1 , ϵ_1 and n_2 , ϵ_2 are the refractive index and the dielectric constant perpendicular and parallel to the polar axis of a BaTiO₃ single crystal, respectively. The subscripts a , q , c , and b refer to the as-deposited amorphous, quasi-amorphous, crystallized, and bulk phases, respectively.

Sample	Refractive index (634 nm)	Birefringence, $n_{\parallel}-n_{\perp}$	Density with respect to bulk, deduced from refractive index	In-plane stress (GPa)	Dielectric constant (static)	Pyroelectricity [nC/(cm ² K), 300 K]
Amorphous	$n_{\perp}=1.97-2.02$	$-(0.002-0.008)$	$\rho_a/\rho_b=0.82-0.84$	$<\pm 0.030$	9–12	<0.01
quasi-amorphous	$n_{\perp}=1.89-1.94$	0.03–0.07	$\rho_q/\rho_b=0.77-0.82$	$-(2.0-2.2)$ (Compressive)	30–32	1–5
After crystallization	$n_{\perp}=1.80-1.85$	0	$\rho_c/\rho_b=0.71-0.74$	$-(0.2-0.6)$ (Compressive)	>150	0.5–5 (after poling)
Bulk BaTiO ₃	$n_1=2.35-2.38$	$n_1-n_2=-(0.03-0.05)$	$\rho_b/\rho_b=1$		$\epsilon_1 > 4000$ $\epsilon_2 \geq 160$ $\bar{\epsilon} > 1200$	20

zation of amorphous BaTiO₃, and (c) the quasi-amorphous phase is polar, whereas the as-deposited amorphous phase is nonpolar.

A. Mass-density evolution of amorphous BaTiO₃

Crystallization of sputtered amorphous BaTiO₃ films has been studied extensively.^{1,2,12,14–19} Nucleation begins within the temperature range of 470–500 °C.^{1,15} However, films crystallized below 700 °C may have a low density due to high porosity and a noticeable dilatation of the lattice.²⁰ Densification accompanied by a noticeable shrinkage and development of a tensile stress starts above 700 °C.^{1,20}

Our experiments with substrate-free films and data on the refractive index of substrate-supported films clearly show the tendency of as-deposited amorphous films to *expand* upon heating. Indeed, the density of the as-deposited amorphous phase, ρ_a , is larger than that of the quasi-amorphous, ρ_q , phase and than that of the crystalline phase, ρ_c : $\rho_a > \rho_q > \rho_c$ (Table I). After crystallites start growing, film density may only increase. This implies that the nucleation of the crystalline phase occurs in some *intermediate amorphous phase* with a density, ρ_i , which is lower than that of the films crystallized below 700 °C: $\rho_i < \rho_c = (0.71-0.74)\rho_b$ (ρ_b is the density of bulk BaTiO₃, Table I, Fig. 5). The as-deposited amor-

phous films have a density of $\rho_a = (0.82-0.84)\rho_b$ and to reach the density of ρ_i they must expand by 10%–14% before nucleation starts. Thus expansion precedes nucleation and is a precondition for nucleation to occur. This is consistent with an earlier suggested theory⁵ that a low-density amorphous layer exists at the interface between an amorphous and a crystalline phase. In view of the above the crystallization path of the BaTiO₃ may be described as shown in Fig. 5.

If there are no external mechanical constraints, as in the case of *substrate-free* amorphous films¹² or fine amorphous flakes,¹⁵ the amorphous phase undergoes volume expansion upon heating until 470 °C. In this temperature range the low-density amorphous intermediate phase is formed. Further heating causes crystallization of this intermediate phase; substrate-free amorphous films always crystallize. *Substrate-supported* films are not free to expand (clamped). The substrate prevents in-plane expansion and permits only out-of-plane expansion, which is limited due to the finite Poisson ratio of the expanding phase. As a result high in-plane compressive stress builds up. Amorphous ionic (and metallic) phases do not support dislocation movement and grain boundary sliding, which are the major mechanisms of stress relaxation in polycrystalline solids.⁴ If the yield stress of the amorphous phase is not reached, the stressed amorphous phase may persist indefinitely without crystallization.

In this view one might expect that no amorphous substrate-supported films should crystallize irrespective of the heat treatment. This is obviously not true. Any real as-

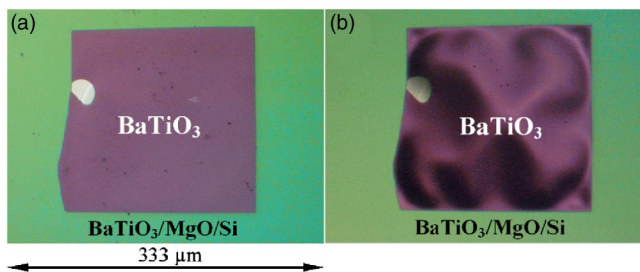


FIG. 4. (Color online) Optical microscopy image (top view) of a 350-nm-thick substrate-free BaTiO₃ film: (a) amorphous as-deposited and (b) after heating at 450 °C for 2 h. The membrane remained noncrystalline, which was verified by wide-angle transmission x-ray scattering (WAXS).

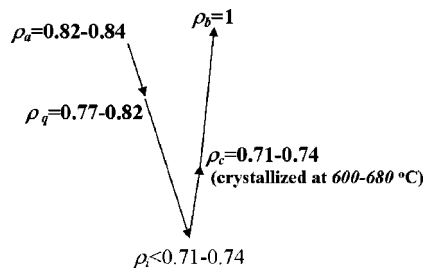


FIG. 5. Density evolution during crystallization of sputtered BaTiO₃ thin films. The density is given relative to a density of a single crystal of BaTiO₃ ($\rho_b=1$).

deposited film has some voids. As the film is heated two competing processes occur: (1) volume expansion that tends to eliminate the free volume of the voids²¹ and (2) nucleation in the regions where the density of the low-density intermediate phase is reached. If the free volume associated with voids is eliminated due to the volume expansion, then no further expansion is possible without stress relaxation and the nucleation is suppressed.

If nucleation begins, then it will proceed, because crystallites provide a very efficient stress relaxation mechanism via grain boundary sliding and dislocation movement. There are three cases in which nucleation can be expected to win: (a) If the *fraction of voids is large*, then volume expansion cannot eliminate all the voids under any conditions and nucleation will proceed. (b) If a film has a *large surface roughness*, then nucleation is unobstructed at the film surface. (c) If the nucleation is heterogeneous, as in the case of the films deposited on a *layer of MgO*, then this layer provides a nucleation (seeding) surface, which is superior to that of Si. The surface of (100) Si does not easily nucleate BaTiO₃ (Refs. 1 and 17) due to the presence of a few monolayers of oxide.²² Further crystal growth on MgO is less affected by external stress due to the presence of the above-mentioned relaxation mechanisms.^{23–25} Therefore, *films with a large number of voids or a rough surface and films deposited on MgO crystallize* irrespective of the thermal treatment.

If the *volume fraction of voids is small*, then the outcome of the competition between volume expansion and nucleation depends on the type of the heat treatment. Under isothermal conditions (600 °C) even films with a small amount of voids will eventually crystallize because nucleation occurs more rapidly than expansion can eliminate voids. When as-deposited amorphous films are pulled through the temperature gradient the temperature increases gradually. Volume expansion of the as-deposited amorphous phase begins at 200 °C—i.e., before the crystalline phase nucleates (>470 °C). When all the free volume is eliminated, then expansion is arrested before the low-density intermediate phase is formed. Then, when the nucleation temperature is reached, nucleation does not occur.

However, slow heating is a necessary but not a sufficient condition for suppression of nucleation. Literature data on crystallization of sputtered BaTiO₃ (Refs. 1, 18–20, 24, and 26–33) do not suggest any retardation of crystallization due to slow temperature ramping. Furthermore, our experiments show that films pulled more slowly than ≈2 mm/h and films pulled faster than 5 mm/h crystallize. Thus the pulling rate is important in the transformation of the amorphous into quasi-amorphous phase. The temperature gradients $\partial T/\partial x \approx 0.01\text{--}0.1\text{ K}/\mu\text{m}$ (Ref. 6) and $\partial T/\partial t \approx 0.01\text{--}0.1\text{ K/s}$ are very small and do not produce any significant thermal stress and strain in thin films of amorphous BaTiO₃.³⁴ However, pulling through the temperature gradient introduces a large *in-plane gradient of stress* because the regions that have already expanded are adjacent to regions that have not yet expanded. The role of this in-plane strain gradient is, probably, twofold. (a) Isomorphic expansion of a substrate-clamped film creates a “plane stress” with axial symmetry. Such a stress field does not have a shear component and cannot lead to elimination of voids^{21,35–37} unless the stress is

very high.^{35,38} Void closure is associated with a change of shape, which appears only due to shear stress.^{21,36,37} Pulling through the temperature gradient breaks the axial symmetry of the stress field and creates stress with a shear component, which leads to the elimination of the voids.³⁵ (b) The in-plane stress gradient introduces anisotropic conditions which cause a poling effect. Without this anisotropy, the transformation of the isotropic as-deposited amorphous films into the polar (pyroelectric) anisotropic quasi-amorphous films would not occur. Thus the *quasi-amorphous phase* is an underexpanded amorphous phase that is formed in a gradient of stress.

B. Estimate of the degree of expansion required to suppress the crystallization

The degree of expansion required to suppress crystallization can be estimated from thermodynamic considerations. Let us consider an infinitely large amorphous phase, in which a spherical region of radius r_0 expands to form the low-density intermediate phase. The change of free energy, $\Delta\mu^{a\rightarrow i}$, during this process is given by

$$\Delta\mu^{a\rightarrow i} = \Delta H^{a\rightarrow i} - T\Delta S^{a\rightarrow i} + A_E, \quad (1)$$

where $\Delta H^{a\rightarrow i}$ is the enthalpy of the of formation of the intermediate phase, $\Delta S^{a\rightarrow i}$ is the change of entropy between the amorphous phase and the low-density intermediate phase, T is temperature, and A_E is the elastic energy associated with the expansion. This energy can be estimated as follows. If a sphere of radius r_0 is removed from the amorphous matrix with a density of ρ_a and expanded to a sphere with the density of the intermediate phase ρ_i , then the radius of this sphere is $\mathbf{r} \approx \mathbf{r}_0(1 + \alpha/3)$, where $\alpha = \rho_a/\rho_i - 1$ is the density mismatch. To return this expanded sphere into the amorphous matrix we have to compress it to a radius r_0 and then let it relax in the amorphous matrix. After the relaxation, the strain inside the sphere is isostatic. If the elastic properties of the matrix and the expanding sphere are similar, then after the relaxation the radius is defined by Lamé’s formulas^{37,39}

$$\mathbf{r} = \mathbf{r}_0 \left(1 + \frac{\alpha}{3} \frac{1}{1 + \gamma} \right), \quad \gamma = \frac{2(1 - 2\nu)}{(1 + \nu)}, \quad (2)$$

where ν is the Poisson ratio. The strain u_{rr} inside the sphere is given by³⁷

$$\mathbf{u}_{rr} = -\frac{\alpha}{3} \frac{\gamma}{\gamma + 1}. \quad (3)$$

The pressure at the surface of a sphere under isostatic stress is³⁶

$$P = 3Bu_{rr}, \quad (4)$$

where B is the bulk modulus of the sphere. One can assume that the amorphous material is isotropic and its mechanical properties are close to those of the crystalline material, $B \approx 115\text{ GPa}$ and $\nu \approx 0.325$.⁴⁰ The work associated with the expansion of the sphere is given by

$$dA_E = -PdV \approx -3Bu_{rr}4\pi r_0^2 dr = BV \frac{\gamma}{(1+\gamma)^2} \alpha d\alpha, \quad (5)$$

where $V = \frac{4}{3}\pi r_0^3$ is the initial volume of the sphere. Integration with respect to α yields

$$A_E = \frac{BV\alpha^2}{2} \frac{\gamma}{(1+\gamma)^2}. \quad (6)$$

From Eq. (6) one can find A_E expressed in J/mol:

$$A_E = \frac{B\alpha^2}{2\rho_a} \frac{\gamma}{(1+\gamma)^2}, \quad (7)$$

where ρ_a is expressed in mol/m³. Strictly speaking, Eq. (7) is valid for an inclusion of the intermediate phase which is much smaller than the film thickness, and because it neglects macroscopic in-plane stresses, it sets a lower limit.

The enthalpy of formation of the intermediate phase, $\Delta H^{a \rightarrow i}$, must be smaller than the enthalpy of transition from the amorphous phase to the crystalline phase, $\Delta H^{a \rightarrow c}$, because formation of the intermediate phase and the subsequent crystallization are successive processes $\Delta H^{a \rightarrow c} = \Delta H^{a \rightarrow i} + \Delta H^{i \rightarrow c}$ (all enthalpies are negative). The crystallization enthalpy of sputtered amorphous BaTiO₃ calculated from the data given in Ref. 15 is $\approx -(7-9)$ kJ/mol. The term $-T\Delta S^{a \rightarrow i}$ [Eq. (1)] is positive and can be neglected because both the amorphous and low-density intermediate phases are noncrystalline, which implies that the entropy difference between them is small. Formation of the intermediate phase becomes highly improbable if $\Delta\mu^{a \rightarrow i} > 0$. Thus,

$$\begin{aligned} \Delta\mu^{a \rightarrow i} &= \Delta H^{a \rightarrow i} - T\Delta S^{a \rightarrow i} + A_E \\ &> \Delta H^{a \rightarrow c} + \frac{B\alpha^2}{2\rho_a} \frac{\gamma}{(1+\gamma)^2} > 0. \end{aligned} \quad (8)$$

Consequently formation of the low-density intermediate phase is rendered impossible if the density mismatch exceeds some critical value α_{cr} :

$$\alpha_{cr} \geq (1+\gamma) \sqrt{\frac{-2\rho_a \Delta H^{a \rightarrow c}}{B\gamma}} = 12.4\%. \quad (9)$$

The inequality in Eq. (9) can be compared with the experimental data. The density of the crystallized films is larger than the density of the intermediate phase, because after crystallization the density may only increase. From the data in Table I one can obtain that $\alpha_{\text{expt}} > \rho_a/\rho_c - 1 = 13\%$ (see Table I, Fig. 5), which is in excellent agreement with the value of α_{cr} obtained from Eq. (9).

There are three comments to be made regarding the above estimate of the density mismatch.

(a) In the case under consideration nucleation is possible only in the intermediate phase, the formation of which is arrested by substrate clamping. Therefore, the size of a ‘‘critical’’ nucleus^{41,42} in a defect-free film is the size which ensures relaxation of the stress; i.e., it must be comparable with the film thickness. Obviously, formation of a nucleus of such a size is highly improbable.

(b) As noted above, the calculation is valid for an infinitely large amorphous matrix, which accumulates elastic

stress if the low-density phase appears. In reality, substrate-supported films are clamped in the x and y directions and can expand freely in the z direction which is perpendicular to the plane of the film (the ‘‘plane stress’’ case³⁶). This expansion decreases the effective density mismatch. The remanent expansion of the films can be estimated from the experimental data on density deduced from refractive index n_{\perp} (Fig. 5 and Table I). The strain in the direction perpendicular to the film plane is

$$u_{zz} \approx \frac{\rho_a - \rho_q}{\rho_a} = 0.04 \approx 0.3\alpha_{\text{expt}}. \quad (10)$$

Under the conditions of biaxial clamping, the relative change of volume is equal to u_{zz} and Eq. (10) shows that the expansion reaches only $\approx 30\%$ of what it would reach in the absence of mechanical constraints. This implies that $\approx 70\%$ of the actual density mismatch α_{expt} required for crystallization is prevented by clamping. Therefore, Eq. (9) provides a fair estimate for the critical value of the density mismatch.

(c) In the complete absence of mechanical constraints the amorphous phase undergoes isomorphic expansion and nucleation is unobstructed once the low density phase is formed. However, if the amorphous phase is perfect—i.e., void free—formation of a small inclusion of a low-density phase inside the amorphous matrix is retarded or suppressed completely irrespective of the boundary conditions and geometrical dimensions.

C. Effect of the temperature gradient on the formation of the quasi-amorphous phase

The effect of pulling the film through the temperature gradient can be qualitatively understood from the following analysis. During pulling, the density becomes a function of position in the film, \mathbf{x} ($x > 0$). Therefore, the stress σ_{xx} and the strain u_{zz} also depend on \mathbf{x} . In the presence of the temperature gradient the stress field is not exactly a plane stress because the shear stress σ_{xz} is not strictly zero. However, if the width of the hot zone L , is much larger than the film thickness d , which is the case here ($L \approx 10^{-1}$ cm⁻¹ and $d < 250$ nm), then $\sigma_{xz} \gg \sigma_{xx} \approx \sigma_{yy}$, and it is justified to use the plane stress approximation^{34,36} to estimate σ_{xx} , σ_{xz} , and u_{zz} . In the absence of mechanical constraints, the amorphous material would undergo volume expansion from a density ρ_a to a density $\rho(T(\mathbf{x}), t)$, where T is the temperature and t is the time which has elapsed from the beginning of the expansion process. Therefore, for the case of biaxial clamping one can write

$$\sigma_{xx} \approx \frac{E}{(1-\nu)} \frac{\rho_a - \rho(T(\mathbf{x}), t)}{3\rho_a} = \beta \frac{\rho_a - \rho(T(\mathbf{x}), t)}{3\rho_a}, \quad (11)$$

where

$$\beta = \frac{E}{(1-\nu)},$$

and from Eq. (10),

$$u_{zz} \approx 0.3 \frac{\rho_a - \rho(\mathbf{T}(\mathbf{x}), t)}{\rho_a} = 0.3 \frac{\rho_a - \rho(\mathbf{T}(\mathbf{x}), t)}{\rho_a}, \quad (12)$$

where E is the Young's modulus (≈ 120 GPa).⁴⁰ Equation (11) can be easily verified by the experimental data. Since the density undergoes a few percent change upon conversion from the amorphous to quasi-amorphous state, the in-plane stress σ_{xx} must be of the order of a few GPa. This matches the stress measured in the quasi-amorphous films of ≈ 2 GPa.

Since the temperature gradient has only an x component, the condition of mechanical equilibrium is³⁶

$$\frac{\partial \sigma_{xx}}{\partial x} + \frac{\partial \sigma_{xz}}{\partial z} = 0 \Rightarrow \sigma_{xz} = - \int \frac{\partial \sigma_{xx}}{\partial x} dz \approx -d \frac{\partial \sigma_{xx}}{\partial x}, \quad (13)$$

where d is the film thickness. Then from Eqs. (12) and (13) one obtains

$$\sigma_{xz}(\mathbf{x}, t) \approx \frac{\beta d}{3\rho_a} \frac{\partial \rho(\mathbf{T}(\mathbf{x}), t)}{\partial x} = \frac{\beta d}{3\rho_a} \frac{\partial \rho(\mathbf{T}(\mathbf{x}), t)}{\partial \mathbf{T}(\mathbf{x})} \frac{\partial \mathbf{T}(\mathbf{x})}{\partial x}. \quad (14)$$

The behavior of $\rho(\mathbf{T}(\mathbf{x}), t)$ is known qualitatively; therefore, Eq. (14) can be easily analyzed. When a film is pulled through the temperature gradient, the rate of expansion of the amorphous phase can be expressed in the most general case as⁴³

$$\frac{\partial \rho(\mathbf{T}, t)}{\partial t} = -f(\rho(\mathbf{T}, t) - \rho_0(\mathbf{T})) \cdot g(\mathbf{T}), \quad (15)$$

where $\rho_0(\mathbf{T})$ is the equilibrium density of the amorphous phase corresponding to the temperature \mathbf{T} . The functions $f(\rho(\mathbf{T}, t) - \rho_0(\mathbf{T}))$ and $g(\mathbf{T})$ describe the influence of the density difference and temperature on the rate of expansion of the film, respectively, and therefore they must be finite, smooth and non-negative. During pulling with rate s the temperature profile is $\mathbf{T} = \mathbf{T}(\mathbf{x} - s\mathbf{t})$. The hot zone is confined to a narrow region, $-L < \mathbf{x} - s\mathbf{t} < 0$, outside which no expansion occurs. Therefore, if $t < \mathbf{x}/s$, the expansion has not yet started and the stress is zero. If the pulling rate is high—i.e., $s \rightarrow \infty$ —then the time available for that material to expand, $L/s \rightarrow 0$, is too short for the expansion to take place. This means that $\rho(\mathbf{T}, t) \rightarrow \rho_a$ everywhere and the stress is zero [Eq. (14)]. If the pulling rate is low ($s \rightarrow 0$), then there is sufficient time for the density to equilibrate and hence in all regions inside the hot zone, $\rho(\mathbf{T}(\mathbf{x}), t) \rightarrow \rho_0(\mathbf{T}(\mathbf{x}))$. In this case Eq. (14) becomes

$$\sigma_{xz}(\mathbf{x}) \approx \frac{\beta d}{3\rho_a} \frac{\partial \rho_0(\mathbf{T}(\mathbf{x}))}{\partial \mathbf{T}(\mathbf{x})} \frac{\partial \mathbf{T}(\mathbf{x})}{\partial x}, \quad (16)$$

where $\partial \rho_0(\mathbf{T})/\partial \mathbf{T}(\mathbf{x})$ is purely a property of the material. Thus, one can see that if the temperature gradient is too steep and/or the pulling rate is too low, then the shear stress is large and may exceed the yield limit of the amorphous films. This would lead to the creation of hillocks where nucleation can begin. Traces of hillocks are clearly visible on the surface of the films crystallized under isothermal conditions.⁶ Thus, from the most general considerations one can conclude

that there are upper and lower limits for both the temperature gradient and the pulling rate such that expansion will take place, but there will be no crystallization. Our experimental parameters ensure that the material is pulled through the hot zone faster than the rate required for the density to reach $\rho_0(\mathbf{T}(\mathbf{x}))$. Consequently, the shear stress must be lower than that given by Eq. (16); however, it is still high enough to eliminate the void volume.

The order of magnitude of σ_{xz} can be estimated from Eq. (13). The in-plane stress σ_{xx} in the amorphous phase is zero, and in the quasi-amorphous phase it is ≈ 2 GPa. The transition region l , where the in-plane stress rises from zero to its maximum value, must be much smaller than the width of the hot zone, $L \approx 10^{-1}$ cm, where the expansion occurs.⁶ Therefore, one can take $l \approx 10^{-2}$ cm. Thus, if the film thickness is $d < 250$ nm,⁶ then from Eq. (13) $\sigma_{xz} > (d/l)\sigma_{xx} \approx 5$ MPa. This is a realistic value which is much lower than the typical yield stress (few hundreds of MPa), but which is sufficiently large to cause collapse of the voids.^{21,35} In agreement with the experimental data⁶ this derivation predicts that there is upper limit on the film thickness, beyond which the films crystallize irrespective of the type of heat treatment.

Extending the above calculation, it is also possible to estimate the gradient of the strain u_{zz} . Similarly to Eqs. (12)–(17) one can write for the maximum value of the strain:

$$\left. \frac{\partial u_{zz}}{\partial x} \right|_{\max} = \frac{0.3}{\rho_a} \left(\frac{\partial \rho_0(\mathbf{T})}{\partial \mathbf{T}(\mathbf{x})} \frac{\partial \mathbf{T}(\mathbf{x})}{\partial x} \right)_{\max}. \quad (17)$$

This strain can be estimated from the following. The strain u_{zz} is zero in the amorphous films and reaches its maximum value of $u_{zz} \approx 0.04$ in the quasi-amorphous films. The width of the region of maximum strain gradient is similar to the width of the region where the stress σ_{xz} is close to maximum, $l \approx 10^{-2}$ cm. Therefore, the strain gradient is

$$\left. \frac{\partial u_{zz}}{\partial x} \right|_{\max} \approx \frac{u_{zz}}{l} = 4 \text{ cm}^{-1}. \quad (18)$$

D. Origin of the poling effect in quasi-amorphous films

The presence of the strong uniaxial strain gradient provides insight into the origin of pyroelectricity in quasi-amorphous films. The as-deposited amorphous films are isotropic, whereas the quasi-amorphous films are, pyroelectric and, therefore, noncentrosymmetric and anisotropic. The density of quasi-amorphous films is close to that of the amorphous ones ($\rho_q/\rho_a \approx 94\% - 100\%$). In addition, the dielectric constants of the amorphous and quasi-amorphous films, though very different (≈ 9 versus ≈ 32), are still much smaller than that of the polycrystalline BaTiO_3 (> 1000). Therefore, one can expect that the structures of quasi-amorphous and amorphous films are closely related; however, the quasi-amorphous films must have regions with some short-range order. In order to exhibit a pyroelectric effect, some fraction of the regions with local order must possess a permanent dipole moment and the angular distribution of the local dipoles must be anisotropic; i.e., the vector sum of the individual dipole moments should not vanish.

Such an arrangement may appear only if the regions with local order are formed under conditions favoring some directions over others. These conditions are created by the uniaxial strain gradient mentioned above. It should be noted that the gradient of strain produces a small spontaneous (flexoelectric) polarization. The poling effect of this polarization is equivalent to a poling effect of an electric field, F ,^{44–47} which can be estimated as^{44,47}

$$F \approx \frac{1}{4\pi\epsilon_0} \frac{\partial u_{zz}}{\partial x} \frac{e}{\delta} = 10^1 - 10^2 \frac{\text{V}}{\text{cm}}, \quad (19)$$

where $\delta \approx 2 \text{ \AA}$ is an interatomic distance, ϵ_0 is the dielectric permittivity of vacuum, and e is the elementary charge. Equations (17)–(19) predict the existence of a strain gradient and an equivalent poling electric field that are in-plane—i.e., perpendicular to the transition front between the amorphous and quasi-amorphous phases. Since the transition region propagates with strongly asymmetric boundary conditions—i.e., a substrate below and a free surface above—the direction of the strain gradient and the electric field must have both in-plane and out-of-plane components. Thus the transformation from the amorphous to the quasi-amorphous state and formation of crystal motifs occur in the presence of a mechanical strain gradient that causes poling. The gradient of the mechanical strain and the flexoelectric effect can be viewed as a primary cause of local crystal motif alignment which gives rise to the pyroelectric effect with an experimentally detectable out-of-plane component.⁶ Such a local alignment is consistent with the increase of the dielectric constant observed during the transition from the amorphous to the quasi-amorphous state. The microscopic origin of polarity in quasi-amorphous BaTiO₃ was recently investigated by extended x-ray absorption fine structure (EXAFS).⁴⁸

V. CONCLUSIONS

The arguments presented above suggest a mechanism that may provide considerable thermal stability for noncrystalline ionic solids. Nucleation of crystalline BaTiO₃ occurs only in

a low-density amorphous intermediate phase that forms as a result of a large volume expansion of the as-deposited amorphous phase. Thus, formation of a low-density intermediate phase is seen as a precondition for nucleation and crystallization. In the absence of external mechanical constraints volume expansion is unobstructed and nucleation proceeds freely. In a thin film clamped by a substrate, volume expansion is restricted and nucleation may be completely suppressed. This indeed occurs if an as-deposited amorphous film is pulled through a temperature gradient. The resulting phase is quasi-amorphous. As long as the mechanical constraints are in place the quasi-amorphous phase retains stability at temperatures that would normally lead to crystallization of sputtered BaTiO₃. The unique properties of the quasi-amorphous phase, including pyroelectricity and piezoelectricity, are determined by a degree of anisotropy associated, most probably, with the presence of regions with short-range order and their partial alignment. This alignment is likely caused by a strain gradient and resulting flexoelectric effect which exist during the transformation of the amorphous as-deposited film to the quasi-amorphous phase.

Two preconditions for the formation and stability of the quasi-amorphous phase are small enthalpy of crystallization and large volume expansion upon heating prior to crystallization. Thus as-deposited films of other amorphous ionic oxides which satisfy these requirements could potentially form the quasi-amorphous state if pulled through a temperature gradient. Variation of mechanical constraints may produce an indefinitely large number of quasi-amorphous phases with different density.

ACKNOWLEDGMENTS

The authors wish to acknowledge the Israel Science Foundation and U.S.-Israel Binational Science Foundation for funding this research. I.Z. thanks the Israeli Ministry of the Immigrant Absorption for partial support. A.T. acknowledges support of INTAS Project No. 01-0818. We express our appreciation to Professor Oscar M. Stafsudd of UCLA for very fruitful discussions.

*Electronic address: Igor.Lubomirsky@weizmann.ac.il

¹W. T. Liu, S. T. Lakshmikumar, D. B. Knorr, E. J. Rymaszewski, T. M. Lu, and H. Bakhr, *Appl. Phys. Lett.* **66**, 809 (1995).

²D. Y. Noh, H. H. Lee, T. S. Kang, and J. H. Je, *Appl. Phys. Lett.* **72**, 2823 (1998).

³L. Addadi, S. Raz, and S. Weiner, *Adv. Mater. (Weinheim, Ger.)* **15**, 959 (2003).

⁴R. Zallen, *The Physics of Amorphous Solids* (Wiley, New York, 1983).

⁵F. Ye and K. Lu, *Phys. Rev. B* **60**, 7018 (1999).

⁶V. Lyahovitskaya, I. Zon, Y. Feldman, S. R. Cohen, A. K. Tagantsev, and I. Lubomirsky, *Adv. Mater. (Weinheim, Ger.)* **15**, 1826 (2003).

⁷J. Aizenberg, G. Lambert, L. Addadi, and S. Weiner, *Adv. Mater. (Weinheim, Ger.)* **8**, 222 (1996).

⁸T. Imura, M. Suwa, and K. Fujii, *Mater. Sci. Eng.* **97**, 247 (1988).

⁹A. A. Lipovskii, D. K. Tagantsev, A. A. Vetrov, and O. V. Yanush, *Opt. Mater. (Amsterdam, Neth.)* **21**, 749 (2003).

¹⁰G. Ayton, M. J. P. Gingras, and G. N. Patey, *Phys. Rev. E* **56**, 562 (1997).

¹¹E. A. Kahn and A. J. Leyendecker, *Phys. Rev.* **135**, A1321 (1964).

¹²N. Stavitski, V. Lyahovitskaya, J. Nair, I. Zon, R. Popovitz-Biro, E. Wachtel, Y. Feldman, and I. Lubomirsky, *Appl. Phys. Lett.* **81**, 4177 (2002).

¹³J. P. Nair, N. Stavitski, I. Zon, K. Gartsman, I. Lubomirsky, and A. L. Roytburd, *Europhys. Lett.* **60**, 782 (2002).

¹⁴P. Li and T. M. Lu, *Appl. Phys. Lett.* **59**, 1064 (1991).

¹⁵J. P. Chu, S. F. Wang, S. J. Lee, and C. W. Chang, *J. Appl. Phys.* **88**, 6086 (2000).

- ¹⁶K. Sreenivas, A. Mansingh, and M. Sayer, *J. Appl. Phys.* **62**, 4475 (1987).
- ¹⁷B. S. Chiou and M. C. Lin, *Thin Solid Films* **248**, 247 (1994).
- ¹⁸H. Kawano, K. Morii, and Y. Nakayama, *J. Appl. Phys.* **73**, 5141 (1993).
- ¹⁹C. V. R. Vasant Kumar, A. Dhar, and A. Mansingh, *Appl. Phys. Lett.* **60**, 947 (1992).
- ²⁰L. Nam-Yang, T. Sekine, Y. Ito, and K. Uchino, *Jpn. J. Appl. Phys., Part 1* **33**, 1484 (1994).
- ²¹N. G. Savin, *Stress Distribution around Holes* (NASA, Washington, DC, 1970).
- ²²A. H. Mueller, N. A. Suvorova, E. A. Irene, O. Auciello, and J. A. Schultz, *Appl. Phys. Lett.* **80**, 3796 (2002).
- ²³F. G. Shi, *J. Appl. Phys.* **76**, 5149 (1994).
- ²⁴J. H. Jou, L. Hsu, S. Yeh, and T. Shyy, *Thin Solid Films* **201**, 69 (1991).
- ²⁵H. Gleiter, *Prog. Mater. Sci.* **33**, 223 (1989).
- ²⁶A. Dazzi, A. Gueldry, M. Maglione, P. Sibillot, P. Mathey, and P. Jullien, *Eur. Phys. J.: Appl. Phys.* **9**, 181 (2000).
- ²⁷E. K. Evangelou, N. Konofaos, and C. B. Thomas, *Philos. Mag. B* **80**, 395 (2000).
- ²⁸J. H. Kim and S. Hishita, *J. Mater. Sci.* **30**, 4645 (1995).
- ²⁹C. V. R. V. Kumar, A. Dhar, and A. Mansingh, *Appl. Phys. Lett.* **60**, 947 (1992).
- ³⁰C. V. R. V. Kumar, R. Pascual, and M. Sayer, *J. Appl. Phys.* **71**, 864 (1992).
- ³¹N. Y. Lee, T. Sekine, Y. Ito, and K. Uchino, *Jpn. J. Appl. Phys., Part 1* **33**, 1484 (1994).
- ³²T. Missana, C. N. Afonso, A. K. Petford-Long, and R. C. Doole, *Philos. Mag. A* **79**, 2577 (1999).
- ³³J. E. Snyder, V. G. Harris, N. C. Koon, X. Sui, and M. H. Kryder, *IEEE Trans. Magn.* **31**, 3844 (1995).
- ³⁴D. J. Johns, *Thermal Stress Analysis* (Pergamon, Oxford, 1965).
- ³⁵R. Abeyaratne and H. S. Hou, *J. Elast.* **26**, 23 (1991).
- ³⁶S. Timoshenko and J. N. Goodier, *Theory of elasticity* (McGraw-Hill, New York, 1970).
- ³⁷H. W. Westergaard, *Theory of elasticity and plasticity* (Harvard University Press, Cambridge, MA, 1952).
- ³⁸Z. Suo and W. Wang, *J. Appl. Phys.* **76**, 3410 (1994).
- ³⁹J. H. Davies, *J. Appl. Phys.* **84**, 1358 (1998).
- ⁴⁰N. A. Pertsev, A. G. Zembilgotov, and A. K. Tagantsev, *Phys. Rev. Lett.* **80**, 1988 (1998).
- ⁴¹F. Rosenberger, *Fundamentals of Crystal Growth* (Springer-Verlag, Berlin, 1979).
- ⁴²H. Pfeiffer, *Microscopic Theory of Crystal Growth* (Akademie-Verlag, Berlin, 1989).
- ⁴³S. R. De Groot and P. Mazur, *Non-Equilibrium Thermodynamics* (Dover, New York, 1984).
- ⁴⁴A. K. Tagantsev, *Phys. Rev. B* **34**, 5883 (1986).
- ⁴⁵W. H. Ma and L. E. Cross, *Appl. Phys. Lett.* **82**, 3293 (2003).
- ⁴⁶W. H. Ma and L. E. Cross, *Appl. Phys. Lett.* **81**, 3440 (2002).
- ⁴⁷A. K. Tagantsev, *Phase Transitions* **35**, 119 (1991).
- ⁴⁸A. Frenkel, Y. Feldman, V. Lyahovitskaya, E. Wachtel, and I. Lubomirsky, *Phys. Rev. B* **71**, 024116 (2005).